

# Dynamics of kicked matter-wave solitons in an optical lattice

A. Cetoli<sup>1</sup>, L. Salasnich<sup>2</sup>, B.A. Malomed<sup>3</sup>, F. Toigo<sup>4</sup>

<sup>1</sup>*Department of Physics, Umeå University, SE-90187 Umeå, Sweden*

<sup>2</sup>*CNISM and CNR-INFN, Unità di Padova, Dipartimento di Fisica “Galileo Galilei”, Università di Padova, Via Marzolo 8, 35131 Padova, Italy*

<sup>3</sup>*Department of Interdisciplinary Studies, School of Electrical Engineering, Faculty of Engineering, Tel Aviv University, Tel Aviv 69978, Israel*

<sup>4</sup>*Dipartimento di Fisica “Galileo Galilei” and CNISM, Università di Padova, Via Marzolo 8, 35131 Padova, Italy*

---

## Abstract

We investigate effects of the application of a kick to one-dimensional matter-wave solitons in a self-attractive Bose-Einstein condensate trapped in an optical lattice. The resulting soliton’s dynamics is studied within the framework of the time-dependent nonpolynomial Schrödinger equation. The crossover from the pinning to quasi-free motion crucially depends on the size of the kick, strength of the self-attraction, and parameters of the optical lattice.

*Key words:* Bose-Einstein condensation, solitons, phase imprinting, periodic potentials, pinning, depinning

*PACS:* 03.75.Hh, 03.75.Kk, 03.75.Lm

---

## 1. Introduction

It is well known that Bose-Einstein condensates (BECs) with repulsive inter-atomic interactions, characterized by a positive scattering length,  $a_s > 0$ , can give rise to stable localized matter-wave states in the form of *gap solitons*, in the presence of an optical lattice (OL), which induces a periodic potential acting on atoms. The existence of gap solitons in BEC was predicted theoretically [1] and demonstrated experimentally [2], see also review [3]. Gap solitons are represented by stationary solutions to the respective Gross-Pitaevskii equation (GPE), with the eigenvalue (chemical potential) located in a finite bandgap of the OL-induced spectrum. Note that a periodic potential emulating the OL can also be induced by the spatially-periodic modulation of the transverse trap which confines the condensate in the transverse directions [4,5].

In the limit of a very deep OL, the underlying GPE can be reduced to an effective 1D discrete nonlinear

Schrödinger equation with the repulsive on-site nonlinearity, assuming that the condensate’s wave function is a superposition of functions localized at particular lattice sites, with a nearly vanishing overlap between them [6]. In this limit, gap solitons go over into *staggered* discrete solitons, which feature the alternation of the sign of the wave field between adjacent sites of the lattice [7]. On the other hand, if the corresponding OL is weak, the general wave function may be split into a superposition of right- and left-traveling modes, giving rise to a system of coupled-mode equations for the respective slowly varying amplitudes (see, e.g., Ref. [8]), which is tantamount to the well-known coupled-mode equations for optical waves propagating through the Bragg grating [9]. Actually, gap solitons were first predicted [10] and experimentally created [11] as optical pulses in fiber Bragg gratings.

While the gap solitons are typically studied as standing localized states, a detailed numerical analysis has demonstrated that an initial kick (repre-

sented by a linear phase profile imprinted into the soliton) may set that them in persistent motion, if the norm of the soliton (the number of atoms bound in it) is below a certain threshold value. The existence of moving gap solitons was predicted in both one- and two-dimensional (1D and 2D) settings [8].

In the BEC with attractive interactions ( $a_s < 0$ ), solitons realize the ground state of the condensate. Such solitons were created in condensates of  $^7\text{Li}$  [12] and  $^{85}\text{Rb}$  [13] atoms, with the sign of the atomic interactions switched to attraction by means of the Feshbach-resonance technique (in the latter case, the solitons were observed in a post-collapse state of the condensate). In the presence of a periodic potential, such solitons should exist too, with the chemical potential falling in the semi-infinite gap of the spectrum, as first shown in the context of the optical setting [14], and later demonstrated in detail in the framework of GPEs [15,16,5].

The objective of this work is to predict possible regimes of motion of the 1D matter-wave solitons in the *self-attractive* condensate, in the presence of the OL potential. This will be done in the framework of the nonpolynomial Schrödinger equation (NPSE), which is known to provide for high accuracy in the description of dynamical properties of solitons supported by the self-attraction. This model is described in Section II, while Section III summarizes the findings. The solitons will be first found as stationary solutions to the NPSE, and then set in motion by suddenly kicking them. Three dynamical regimes will be identified by systematic simulations: steady motion, gradual decay of the moving solitons, and firm pinning, when the kick cannot essentially disturb the initial soliton. In particular, regions where these regimes occur will be charted in a parameter plane of the model. The paper is concluded by a brief summary in Section IV.

## 2. Bright solitons in the optical lattice

Dynamics of atomic matter waves in rarefied BEC is very accurately described by the time-dependent three-dimensional GPE,

$$i\hbar\frac{\partial}{\partial t}\psi = \left[-\frac{\hbar^2}{2m}\nabla^2 + U(\mathbf{r}) + \frac{4\pi\hbar^2 a_s}{m}|\psi|^2\right]\psi, \quad (1)$$

where  $\psi(\mathbf{r}, t)$  is the macroscopic wave function of the condensate (normalized to the total number of atoms,  $N$ ),  $m$  the atomic mass, and  $a_s$  the  $s$ -wave scattering length of the inter-atomic potential. As

the trapping potential, we adopt the usual combination of the tight confinement in the radial direction and longitudinal OL,

$$U(\mathbf{r}) = (1/2)m\omega_\perp^2(x^2 + y^2) + V(z), \quad (2)$$

$$V(z) = -V_0 \cos(2k_L z), \quad (3)$$

with  $k_L = 2\pi/\lambda$ , where  $\lambda$  is the wavelength of counterpropagating laser beams whose interference creates the OL, and  $V_0$  is its effective depth. In the subsequent analysis, we use the effective one-dimensional NPSE, which can be derived from Eq. (1) by averaging in the transverse plane [29]. The NPSE has been demonstrated to be very accurate in reproducing results that can be obtained from the full 3D GPE; in particular, this approach has been tested for bright [17] and dark solitons [18], two-component condensates [20], and for the condensate in a toroidal trap [19], as well as for states with axial vorticity [21]. A similar approach, which generalizes the Thomas-Fermi approximation and may give still more accurate results, but does not apply to solitons, was later developed for tightly confined self-repulsive condensates [22].

The NPSE including axial OL potential (3) was derived too [16,5], assuming the following factorization of the 3D wave function in Eq. (1),

$$\psi(\mathbf{r}) = \exp\left\{-\frac{(x^2 + y^2)}{2\sqrt{1 - g|f(z)|^2}}\right\} \frac{f(z)}{(1 - g|f(z)|^2)^{1/4}}, \quad (4)$$

where 1D wave function  $f(z, t)$  is subject to normalization

$$\int |f(z)|^2 dz = 1, \quad (5)$$

the adimensional interaction strength is  $g = 2|a_s|N/a_\perp$ , with  $a_\perp = \sqrt{\hbar/(m\omega_\perp)}$  the transverse trapping size. The respective NPSE takes the form

$$i\frac{\partial f(z, t)}{\partial t} = \left[-\frac{1}{2}\frac{\partial^2}{\partial z^2} + V(z) + \frac{1 - (3/2)g|f(z, t)|^2}{\sqrt{1 - g|f(z, t)|^2}}\right]f(z, t), \quad (6)$$

with length and energy measured in units of  $a_\perp$  and  $\hbar\omega_\perp$ , respectively.

If applied to the ring-like (toroidal) geometry, Eq. (6) predicts that there exists a critical value,  $g_{\min}$ , above which the axially uniform state in the torus becomes modulationally unstable, and is replaced, as the ground state, by a soliton-like configuration.

Moreover, there is another critical value of the interaction strength,  $g_{\text{coll}}$ , above which the localized soliton ceases to exist due to the collapse, hence the soliton persists in interval  $g_{\text{min}} < g < g_{\text{coll}}$ . Similar effects in the toroidal setting were earlier studied in Refs. [23].

Both the full three-dimensional GPE and its NPSE reduction are mean-field equations. Contrary to the repulsive case, in the attractive case that we are dealing with, there is no superfluid-Mott insulator transition. Beyond-mean-field effects are irrelevant in our case too, since, as shown in Ref. [24], they appear at lattice sites populated with a small number of particles ( $\leq 5$ ). In our case, due to the attractive interaction, most of the atoms reside in few highly populated sites.

As concerns quantum effects, it may be relevant to mention that, unlike regular solitons in attractive condensates, gap solitons in the BEC with repulsion cannot represent the ground state. Therefore, in the framework of the full quantum description, the stability of such states needs further analysis. In particular, it was demonstrated that dark solitons in BEC with repulsive interactions between atoms are subject to quantum depletion, with incoherent atoms gradually filling the dark-soliton's notch under the action of anomalous fluctuations [25]. Nevertheless, dark solitons, which accurately obey the mean-field description provided by the GPE, were successfully observed in the experiment [26]. Because loosely bound gap solitons may feature a set of notches in their "tails", they may also be subject to the quantum depletion, in that sense. In terms of the quantum theory, this remains an open question, but the experimental results [2,3] clearly demonstrate that gap solitons can be created, following the predictions of the mean-field theory. On the other hand, for tightly bound soliton in the attractive BEC (as well as for tightly gap solitons in the repulsive condensate, if they are created not too close to edges of the respective bandgap [27]), the quantum depletion should not be an issue, as their existence is not predicated on the presence of notches.

### 3. Phase imprinting and ensuing dynamics

As said above, the objective of this work is to analyze the dynamics of moving bright solitons in the model introduced above, which includes the periodic OL potential. The motion will be initiated by sudden application to the soliton of a kick with mo-

mentum  $p$ .

First, we generate a stationary soliton by numerically solving the corresponding stationary equation, obtained from Eq. (6) by the substitution of  $f(z, t) = e^{-i\mu t}\phi(z)$ , where  $\mu$  is the real chemical potential and  $\phi(z)$  a real stationary wave function:

$$\left[ -\frac{1}{2} \frac{d^2}{dz^2} + V(z) + \frac{1 - (3/2)g\phi^2}{\sqrt{1 - g\phi^2}} \right] \phi(z) = \mu \phi(z). \quad (7)$$

We fix  $k_L \equiv 1$  in potential (3), and solve Eq. (7) with periodic boundary conditions,  $f(z) \equiv f(z + L)$ , with the total length of the ring-shaped system equivalent to 32 periods of the OL,  $L = 32\pi$ . Taking  $V_0 = 0.5$  for the OL depth, we find the ground state of Eq. (7) by means of the numerical scheme described in Refs. [16,5], for values of the interaction strength  $g$  belonging to the above-mentioned existence range,  $g_{\text{min}} < g < g_{\text{coll}}$ .

To initiate the dynamics, we multiply the so determined stationary solution  $\phi(z)$  by  $\exp(ipz)$ , i.e., use the following initial configuration,

$$f(z, t = 0) = \phi(z) \exp(ipz), \quad (8)$$

where momentum  $p$  is compatible with the periodic boundary conditions, taking values  $p = n/16$  with integer  $n$ . We pick up such values in interval  $0 < p < 0.5$ . Configuration (8) can be created in the experiment by means of the well-known phase-imprinting technique [30]. The full time-dependent NPSE, Eq. (6), with initial condition (8), was solved using the Crank-Nicholson predictor-corrector algorithm in real time [31].

Examples of the simulated evolution are displayed in Fig. 1, which suggests the existence of different regimes corresponding to different values of interaction strength  $g$ . In particular, for small  $g$  ( $g = 0.15$ ), the stationary soliton extends over many lattice cells and, after receiving the kick, it moves in quite a regular way. At intermediate values of the interaction strength,  $g = 0.5$ , the soliton occupies a few sites, and its dynamics generated by the action of the kick is irregular. For a larger strength,  $g = 0.8$ , the initial wave packet is essentially localized in a single cell of the lattice, and stays trapped in the same cell (for the entire period of our simulation) after the application of the kick.

To characterize the motion of the kicked soliton in a more accurate form, we calculate the average axial position of the soliton,  $z_0(t) = \int dz z |f(z, t)|^2$ , and its average squared width,

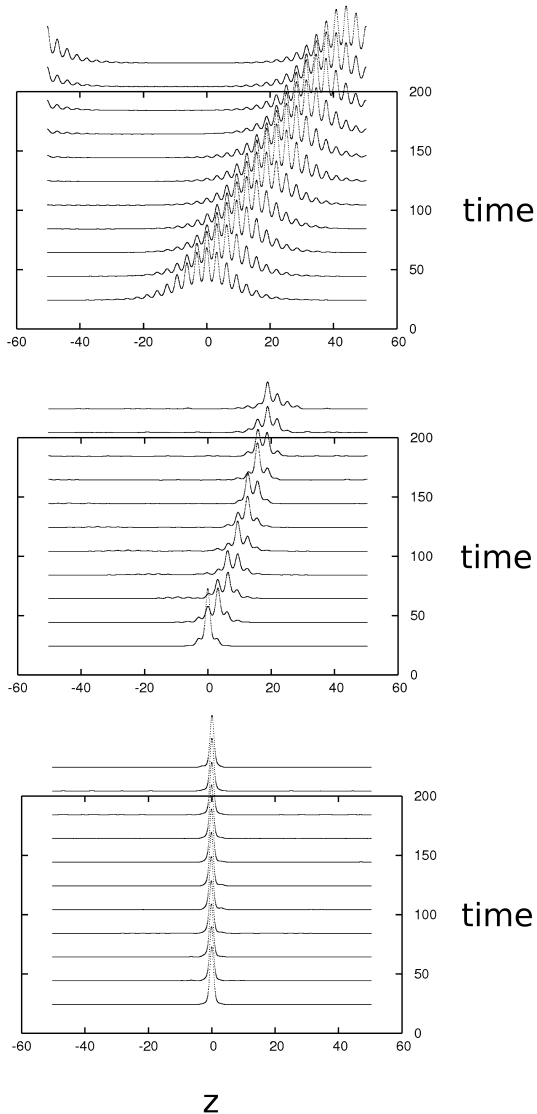


Fig. 1. Profiles  $|f(z, t)|^2$  observed in the course of the evolution of the kicked soliton, with initial momentum  $p = 0.25$ . From top to bottom:  $g = 0.15$ ,  $g = 0.5$  and  $g = 0.8$ . Here and in other figures, parameters of the optical lattice are  $k_L = 1$  and (unless specified otherwise)  $V_0 = 0.5$ .

$$\langle z^2(t) \rangle = \int dz (z - z_0(t))^2 |f(z, t)|^2, \quad (9)$$

where the integration is performed over spatial period  $L \equiv 32\pi$  (the expressions are not divided by the norm of the wave function because it is fixed to be 1, as per Eq. (5)). These characteristics are shown, as functions of time, in Fig. 2 for the same values of  $g$  as in Fig. 1. The figure shows that, with  $g = 0.15$ , the soliton's center of mass ( $z_0$ ) moves at

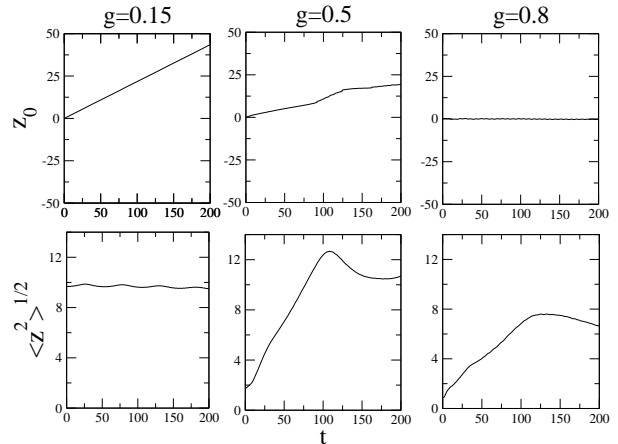


Fig. 2. The center of mass,  $z_0$ , and average axial width,  $\langle z^2 \rangle^{1/2}$ , of the soliton as functions of time. The initial momentum is  $p = 0.25$ .

a constant speed. We have verified that the respective speed is well fitted by expression  $v = p/m^*$ , with the effective inverse mass of the ground state,  $1/m^* = 1 - V_0^2/2$ , as predicted by the usual theory of the quasi-momentum in periodic lattices [32]. Simultaneously, the width of the soliton,  $\sqrt{\langle z^2 \rangle}$ , displays periodic small-amplitude oscillations, i.e., the moving soliton behaves as a *breather*. At  $g = 0.5$ , the motion of the soliton is less regular: its velocity is not constant, and the width increases in the course of the evolution, i.e., the soliton gradually spreads out; however, after becoming much broader than it was initially (by a factor  $\sim 6$ ), it seems to stabilize itself. At  $g = 0.8$ , the initial width of the soliton,  $\sqrt{\langle z^2(t=0) \rangle}$ , is, as said above, comparable to the size of the lattice cell. In this case, the soliton's center of mass does not exhibit any systematic motion, while the width initially increases (by a factor  $\sim 4$ ), but then ceases to grow.

Thus, we do not observe complete delocalization in the regime of spreading. Instead, it is concluded that the soliton interacts with the OL in a complex way, emitting small-amplitude waves, which affect the time evolution of the average width. Figure 3 shows the soliton's profile at  $t = 108$  in the case corresponding to the central panel of Fig. 1, which features the maximum value of  $\sqrt{\langle z^2 \rangle}$ . The figure demonstrates the presence of “splinters”, to the left of the soliton, which actually break off from the soliton shortly after the application of the initial kick. They travel backwards with respect to the soliton, reaching the largest distance from it at  $t = 108$ , due to the periodic boundary conditions. In this situation, expression (9) does not provide an adequate

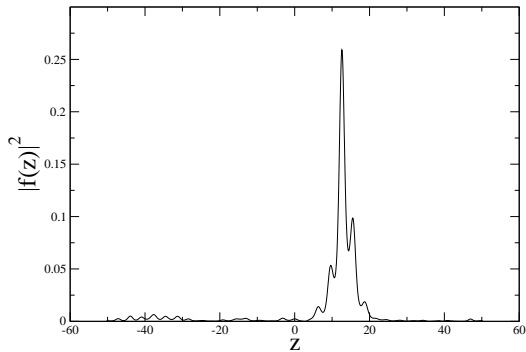


Fig. 3. Snapshot of  $|f(z, t)|^2$  at  $t = 108$  for the soliton in the central panel of Fig. 1, which corresponds to the largest value of  $\langle z^2 \rangle^{1/2}$

measure to estimate the spreading of the soliton. In principle, after performing a round trip in the toroidal trap, the splinters may hit the soliton, but the study of this issue requires extremely long simulations, which we did not perform in the framework of the present work.

As a better measure of the spreading, we introduce the following *effective entropy*,

$$S(t) = - \sum_n A_n(t) \frac{\ln A_n(t)}{\ln(N_{\text{cell}})}, \quad (10)$$

where  $A_n(t)$  is the share of the norm located, at time  $t$ , within the  $n$ -th lattice cell, i.e.  $A_n(t) = \int_{\pi n}^{\pi(n+1)} dz |f(z, t)|^2$ , and  $N_{\text{cell}}$  is the total number of cells [recall we run the simulations for  $N_{\text{cell}} = 32$ , and  $\sum_{n=1}^{N_{\text{cell}}} A_n = 1$ , due to normalization condition (5)]. Definition (10) yields the maximum of the entropy,  $S = 1$ , if the matter is distributed uniformly,  $f(z, t) = \text{const}$ , and the entropy attains its minimum,  $S = 0$ , if the entire norm is concentrated in a single cell.

We have found that the unnormalized effective entropy, i.e.  $S(t) \ln(N_{\text{cell}})$ , turns out to be practically independent of the total length of the system in the axial direction. In particular, while the mean-square width is affected by the backscattered radiation emitted after the kick, the entropy is not. More precisely, we have checked that the result of the computation of the unnormalized entropy does not change with the variation of the total lengths.

In Fig. 4 we plot  $S(t)$  as a function of time for the same runs which were included in Fig. 2. It is seen that, for  $g = 0.15$ , initial entropy  $S(0)$  is large, because the soliton covers many cells, and, in the course of the evolution,  $S(t)$  exhibits periodic small-amplitude oscillations around  $S(0)$ . On the contrary,

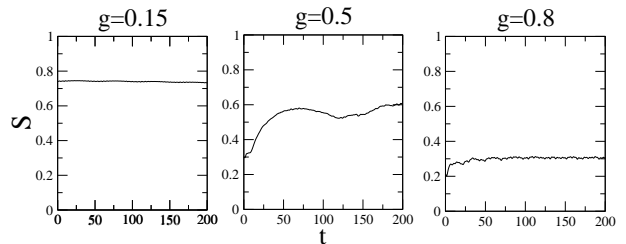


Fig. 4. The same cases as in Fig. 2 are shown here in terms of the evolution of entropy (10).

for  $g = 0.5$  the stationary soliton covers few cells, hence initial entropy  $S(0)$  is quite small, but the entropy increases as a consequence of the soliton's spreading out. For  $g = 0.8$ , the initial entropy is similar to that in the case of  $g = 0.5$ , but its evolution is completely different, featuring very small aperiodic oscillations around  $S(0)$ , i.e.  $S(t)$  remains nearly constant, as the narrow strongly pinned soliton does not start conspicuous motion or spreading out after being kicked.

Thus, our systematic simulations reveal the existence of three different dynamical regimes: (i) stable breathers, i.e., solitons steadily moving across the lattice potential at an almost constant velocity, with small-amplitude shape oscillations; (ii) dispersive dynamics, in which case the soliton strongly spreads out in the course of the evolution; (iii) localization, in which a narrow soliton remains trapped in one lattice cell. In Fig. 5, we plot the respective diagram in the parameter plane of  $(p, g)$ , where these three regimes are mapped as follows.

(i) The black region represents steadily traveling solitons, whose effective entropy varies by  $\leq 5\%$  in the course of the long evolution.

(ii) The gray region: the dispersive regime, in which the solitons move at a variable speed, and their effective entropy increases by more than  $5\%$  against the initial value.

(iii) The white region: localized solitons, with the center of mass firmly pinned to the initial position. In the latter case, the solitons may be slightly dispersive at the initial stage of the evolution, but their effective entropy is always much smaller than in the other two cases.

Figure 5 summarizes results of 560 numerical runs, with 16 values of  $p$  and 35 values of  $g$ . The momentum resolution is imposed by the periodic boundary conditions:  $\Delta p = 2\pi/L$ , where  $L \equiv 32\pi$  is the total axial length, as defined above. By choosing larger  $L$ , one can reduce  $\Delta p$ . The step in the variation of strength  $g$  in Fig. 5 is  $\Delta g = 0.25$ .

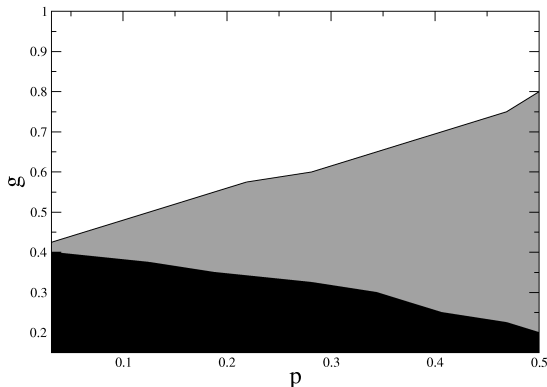


Fig. 5. The map of different dynamical regimes in the plane of  $(p, g)$ , where  $p$  is the momentum imparted to the soliton by the initial kick, and  $g$  the strength of the self-attractive nonlinearity. The black region: steadily moving breather-like solitons; the gray region: spreading out of irregularly moving solitons; the white region: firm pinning (the soliton does not start progressive motion). Lattice parameters:  $V_0 = 0.5$  and  $k_L = 1$ .

Figure 5 shows that the regime of the stable motion is confined to the region of small values of interaction strength  $g$ . For fixed  $g$ , a transition from the steady motion to the dispersive regime is observed with the increase of kick  $p$ , and the numerical results suggest that the steady-motion region disappears as  $p$  attains large values. As expected, the increase of  $g$  drives the system into the regime of pinning, but one can leave it by increasing the kick.

It should be stressed that, while the border between the localization and other two regimes is well defined, the exact location of the boundary between the steady-motion and dispersive regimes depends on our choice of the 5% maximum for the allowed change of the entropy in the course of the evolution. Admitting a 10% change does not conspicuously affect the location of the border, but defining the threshold of 20% makes the region of the stable motion slightly larger (not shown here in detail).

At the boundary between motion and dispersion regimes, we observe a density profile that becomes more and more noisy, while the velocity of the traveling soliton decreases in an irregular way, similar to some regimes of the motion of gap solitons in the 1D model with the repulsive cubic nonlinearity, which were reported in Ref. [8]. This drop in the velocity is also relevant to the identification of the boundary of the pinning regime, where, typically, the kicked soliton visits a few lattice sites and then stops. For instance, at  $g = 0.55$  and  $k = 0.25$ , the soliton passes a few sites, then bounces back to the original posi-

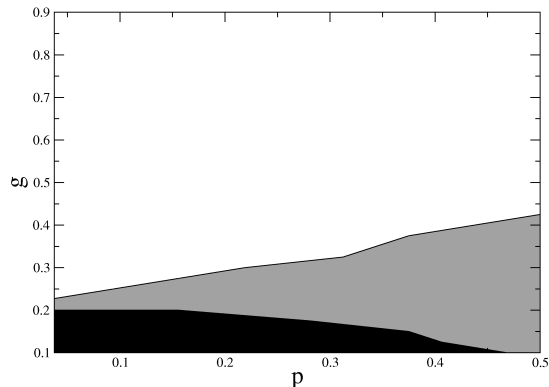


Fig. 6. The same as in Fig. 5, but for  $V_0 = 1$ .

tion, and stays pinned there.

The diagram of the dynamical regimes depends on parameters of the optical lattice,  $V_0$  and  $k_L$ , see Eq. (3). In particular, Fig. 6, obtained by collecting results of other  $16 \times 33 = 528$  numerical runs, displays this diagram for a stronger lattice, with  $V_0 = 1$ , while the OL period remains equal to  $\pi$  (i.e.,  $k_L = 1$ ). Qualitatively, the picture is similar to that shown in Fig. 5, but there are apparent quantitative differences. In particular, the regions of the stable motion and dispersive behavior are strongly reduced, which is not surprising, as the deeper OL can pin the solitons stronger. In addition, the figure shows that there exists a critical momentum,  $p_c$ , above which the region of steady motion does not exist anymore. This critical value  $p_c$  decreases with the increase of OL depth  $V_0$ .

As mentioned above, the upper bound for the considered values of the interaction strength,  $g$ , is imposed by the onset of the collapse,  $g = g_{\text{coll}}$ . In particular, in Ref. [16] it was found that  $g_c = 1.07$  for  $V_0 = 0.5$ , and  $g_{\text{coll}} = 0.96$  for  $V_0 = 1$  (if  $k_L = 1$  is fixed). On the other hand, the minimum strength above which soliton states exist is  $g_{\text{min}} \sim \pi^2/L$  [23]; in this work, this border does not manifest itself, as we considered values of  $g$  at which the soliton is well localized within the lattice; in fact, we always took  $\sqrt{\langle z^2(0) \rangle} < L/10$ .

In an attempt to understand the behavior of the kicked soliton in analytical terms, we tried a variational approach. Using a Gaussian *ansatz*, we derived the respective variational equations of motion. We have thus obtained a set of equations equivalent to that recently reported in Ref. [33]. However, a careful analysis demonstrates that this approach fails to describe the soliton's dynamics correctly in the present model: although it does predict regions

of pinning, moving breathers, and solutions whose width expands indefinitely, the resulting diagram is quite different from those in Figs. 5 and 6. This problem might be expected, since, even in the static case, the Gaussian ansatz does not reproduce the behavior revealed by numerical solutions [16].

#### 4. Conclusions

We have studied the dynamics of moving matter-wave solitons in the self-attractive BEC trapped in the axial optical-lattice potential. The dynamics was induced by kicking a stationary soliton via the phase imprinting. We have performed systematic simulations of the time-dependent nonpolynomial Schrödinger equation, which accurately describes Bose-Einstein condensates under the tight transverse confinement.

Three dynamical regimes have been identified. The first of them is the steady motion of stable solitons with small-amplitude intrinsic oscillations, which is observed at relatively small values of the strength of the inter-atomic attraction  $g$ , and relatively small size of the kick  $p$ , and the second is the dispersive regime, in which the soliton's velocity decreases irregularly, while the soliton suffers systematic spreading. The latter outcome of the application of the kick to the soliton also occurs for relatively small  $g$ , but at larger  $p$ . The third regime naturally features firm pinning, at large values of  $g$  and small  $p$ . A somewhat similar description for dynamical regimes was elaborated in Ref. [6], but the position of the different regions in the respective parameter plane is totally different, due to the fact that the quasi-discrete limit considered in that work is not adequate for comparison with the present model.

Available experimental techniques [12,13] make the experimental realization of the predicted dynamical regimes quite feasible. It may also be relevant, for the purposes of the theory and plausible experiment alike, to study in details collisions between steadily moving solitons. The latter problem will be considered elsewhere.

#### Acknowledgements

This work has been partially supported by Fondazione CARIPARO. B.A.M. appreciates hospitality of the Department of Physics "Galileo Galilei"

at the University of Padova (Padua). L.S. thanks GNFM-INdAM for partial support.

#### References

- [1] F. Kh. Abdullaev, B. Baizakov, S. Darmanyan, V. Konotop, M. Salerno, Phys. Rev. A **64**(2001) 043606; I. Carusotto, D. Embiraco, G. C. La Rocca, *ibid.* **65** (2002) 053611; P. J. Y. Louis, E. A. Ostrovskaya, C. M. Savage, Y. S. Kivshar, *ibid.* **67** (2003) 013602.
- [2] B. Eiermann, Th. Anker, M. Albiez, M. Taglieber, P. Treutlein, K.-P. Marzlin, M. K. Oberthaler, Phys. Rev. Lett. **92** (2004) 230401.
- [3] O. Morsch, M. Oberthaler, Rev. Mod. Phys. **78** (2006) 179.
- [4] S. De Nicola, B. A. Malomed, R. Fedele, Phys. Lett. A **360** (2006) 164.
- [5] L. Salasnich, A. Cetoli, B. A. Malomed, F. Toigo, L. Reatto, Phys. Rev. A **76** (2007) 013623.
- [6] A. Trombettoni, A. Smerzi, Phys. Rev. Lett. **86** (2001) 2353; G. L. Alfimov, P. G. Kevrekidis, V. V. Konotop, M. Salerno, Phys. Rev. E **66** (2002) 046608; A. Smerzi, A. Trombettoni, Phys. Rev. A **68** (2003) 023613.
- [7] P. G. Kevrekidis, K. Ø. Rasmussen, A. R. Bishop, Int. J. Mod. Phys. B **15** (2001) 2833.
- [8] H. Sakaguchi, B.A. Malomed, J. Phys. B: At. Mol. Opt. Phys. **37** (2004) 1443; 2225.
- [9] W. Chen, D. L. Mills, Phys. Rev. Lett. **58** (1987) 160; D. L. Mills, S. E. Trullinger, Phys. Rev. B **36** (1987) 947.
- [10] A. B. Aceves, S. Wabnitz, Phys. Lett. A **141** (1989) 37; D. N. Christodoulides, R. I. Joseph, Phys. Rev. Lett. **62** (1989) 1746.
- [11] B. J. Eggleton, R. E. Slusher, C. M. de Sterke, P. A. Krug, J. E. Sipe, Phys. Rev. Lett. **76** (1996) 1627; B. J. Eggleton, C. M. de Sterke, R. E. Slusher, J. Opt. Soc. Am. B **16** (1999) 587; J. T. Mok, C. M. de Sterke, I. C. M. Littler, B. J. Eggleton, Nature Phys. **2**(2006) 775.
- [12] K. E. Strecker, G.B. Partridge, A. G. Truscott, R. G. Hulet, Nature **417** (2002) 150; L. Khaykovich, F. Schreck, G. Ferrari, T. Bourdel, J. Cubizolles, L. D. Carr, Y. Castin, C. Salomon, Science **296** (2002) 1290.
- [13] S. L. Cornish, S. T. Thompson, C. E. Wieman, Phys. Rev. Lett. **96** (2006) 170401.
- [14] B. A. Malomed, Z. H. Wang, P. L. Chu, G. D. Peng, J. Opt. Soc. Am. B **16** (1999) 1197.
- [15] G. L. Alfimov, V. V. Konotop, M. Salerno, Europhys. Lett. **58** (2002) 7.
- [16] L. Salasnich, A. Cetoli, B. A. Malomed, F. Toigo, Phys. Rev. A **75** (2007) 033622.
- [17] L. Salasnich, A. Parola, L. Reatto, Phys. Rev. A **66** (2002) 043603; L. Salasnich, A. Parola, L. Reatto, Phys. Rev. Lett. **91** (2003) 080405; L. Salasnich, Phys. Rev. A **70** (2004) 053617.
- [18] L. Salasnich, A. Parola, L. Reatto, J. Phys. B: At. Mol. Opt. Phys. **39** (2006) 2839.
- [19] A. Parola, L. Salasnich, R. Rota, L. Reatto, Phys. Rev. A **72** (2005) 063612; L. Salasnich, A. Parola, L. Reatto, Phys. Rev. A **74** (2006) 031603.

- [20] L. Salasnich, B.A. Malomed, Phys. Rev. A **74** (2006) 053610.
- [21] L. Salasnich, B.A. Malomed, F. Toigo, Phys. Rev. A **76** (2007) 063614.
- [22] A. M. Mateo, V. Delgado, Phys. Rev. A **74** (2006) 065602; **75** (2007) 063610.
- [23] L. D. Carr, C. W. Clark, W. P. Reinhardt, Phys. Rev. A **62** (2000) 063611; G. M. Kavoulakis, Phys. Rev. A **67** (2003) 911691; R. Kanamoto, H. Saito, M. Ueda, Phys. Rev. Lett. **94** (2005) 090404.
- [24] N. Oelkers, J. Links, Phys. Rev. B **75** (2007) 115119.
- [25] J. Dziarmaga and K. Sacha, Phys. Rev. A **66** (2002) 043620.
- [26] S. Burger, K. Bongs, S. Dettmer, W. Ertmer, K. Sengstock, A. Sanpera, G. V. Shlyapnikov, M. Lewenstein, Phys. Rev. Lett. **83** (1999) 5198; J. Denschlag, J. E. Simsarian, D. L. Feder, C. W. Clark, L. A. Collins, J. Cubizolles, L. Deng, E. W. Hagley, K. Helmerson, W. P. Reinhardt, S. L. Rolston, B. I. Schneider, W. D. Phillips, Science **287** (2000) 97.
- [27] S. K. Adhikari, B. A. Malomed, Phys. Rev. A **77** (2008) 023607.
- [28] W. Zwerger, J. Opt. B: Quantum Semiclass. Opt. **5**, S9 (2003).
- [29] L. Salasnich, Laser Phys. **12**, 198 (2002); L. Salasnich, A. Parola, L. Reatto, Phys. Rev. A **65**, 043614 (2002).
- [30] J. Denschlag, J. E. Simsarian, D. L. Feder, C. W. Clark, L. A. Collins, J. Cubizolles, L. Deng, E. W. Hagley, K. Helmerson, W. P. Reinhardt, S. L. Rolston, B. I. Schneider, W. D. Phillips, Science **287** (2000) 97.
- [31] E. Carbonechi, R. Mannella, E. Arimondo, L. Salasnich, Phys. Lett. A **249** (1998) 495; L. Salasnich, A. Parola, L. Reatto, Phys. Rev. A **64** (2001) 023601.
- [32] N. W. Ashcroft, N. D. Mermin, *Solid State Physics* (Brooks Cole: Philadelphia, 1976).
- [33] N.H. Berry, J. N. Kutz, Phys. Rev. E **75** (2007) 036214.